A Novel Approach For Hybrid-Electric Power Plants

N.V.S Rakesh kumar
PG Student,
CMRCET

G. Devadas
Professor,
CMR College of Eng. & Technology

K. Chandrashekar reddy
Assistant Professor,
CMR College of Eng & Technology

Abstract—Environmentally friendly solutions are becoming more prominent than ever as a result of concern regarding the state of our deteriorating planet. This paper presents a new system configuration of the front-end rectifier stage for a hybrid wind/photovoltaic energy system. This configuration allows the two sources to supply the load separately or simultaneously depending on the availability of the energy sources. The inherent nature of this Cuk-SEPIC fused converter, additional input filters are not necessary to filter out high frequency harmonics. Harmonic content is detrimental for the generator lifespan, heating issues, and efficiency. The fused multi input rectifier stage also allows Maximum Power Point Tracking (MPPT) to be used to extract maximum power from the wind and sun when it is available. An adaptive MPPT algorithm will be used for the wind system and a standard perturb and observe method will be used for the PV system. A new Operational analysis of the proposed system will be discussed in this paper. Simulation results are given to highlight the merits of the proposed circuit.

Keywords-MPPT, CUK-SEPIC CONVERTERS, PV & *WIND SOURCE*

I. INTRODUCTION

With increasing concern of global warming and the depletion of fossil fuel reserves, many are looking at sustainable energy solutions to preserve the earth for the future generations. Other than hydro power, wind and photovoltaic energy holds the most potential to meet our energy demands. Alone, wind energy is capable of supplying large amounts of power but its presence is highly unpredictable as it can be here one moment and gone in another. Similarly, solar energy is present throughout the day but the solar irradiation levels vary due to sun intensity and unpredictable shadows cast by clouds, birds, trees, etc. The common inherent drawback of wind and photovoltaic systems are their intermittent natures that make them of the systems in literature use a separate DC/DC boost converter connected in parallel in the rectifier stage as shown in Figure 1 to perform the MPPT control for each of the renewable energy power sources. A simpler multi input structure has been suggested that combine the sources from the DC-end while still achieving MPPT for each renewable source. The structure proposed is a fusion of the buck and buck-boost converter. The systems in literature require passive input filters to remove the high frequency current harmonics injected into wind turbine generators. The harmonic content in the generator current decreases its lifespan and increases the power loss due to heating.

In this paper, an alternative multi-input rectifier structure is proposed for hybrid wind/solar energy systems. The proposed design is a fusion of the Cuk and SEPIC converters. The features of the proposed topology are: 1) the inherent nature of these two converters eliminates the need for separate input filters for PFC 2) it can support step up/down operations for each renewable source (can support wide ranges of PV and wind input); 3) MPPT can be realized for each source; 4) individual and simultaneous operation is supported. The circuit operating principles will be discussed in this paper. Simulation results are provided to verify with the feasibility of the proposed system
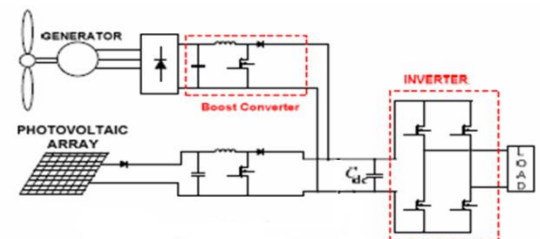

Fig 1: Hybrid system With Multi Connected Boost Converter

II. PROPOSED MULTI-INPUT RECTIFIER STAGE

A system diagram of the proposed rectifier stage of a hybrid energy system is shown in Figure 2, where one of the inputs is connected to the output of the PV array and the other input connected to the output of a generator. The fusion of the two converters is achieved by reconfiguring the two existing diodes from each converter and the shared utilization of the Cuk output inductor by the SEPIC converter. Thisapplications. Also, the converter has high current peaks, which lead to high conduction losses. An attempt to minimize the total number of components in multiple input dc–dc converters has been presented in [15].But neither bi-directional-power-flow capability, nor isolation is provided. Similarly, multiple-energy source-conversion topologies have been presented in [16]. Although, the topology is capable of interfacing sources of different voltage/current characteristics to a common load and achieving a low part count, the $M1$ an $M2$, then the switching states will be state I, II, IV. Similarly, the switching states will be state I, III, IV if the switch conduction periods are vice versa. To provide a better explanation, the inductor current waveforms of each switching state are given as follows assuming that $d2 > d1$; hence only states I, III, IV are discussed in this example. In the following, Ii,PV is the average input current from the PV source;

Ii,W is the RMS input current after the rectifier (wind case); and *Idc* is the average system output current. The key waveforms that illustrate the switching states in this example are shown in Figure 6. The mathematical expression that relates the total output voltage and the two input sources will be illustrated in the next section.

State I (M_1 on, M_2 on):

$$i_{L1} = I_{i,PV} + \frac{V_{PV}}{L_1}t \qquad 0 < t < d_1 T_s$$

$$i_{L2} = I_{dc} + \left(\frac{v_{c1} + v_{c2}}{L_2}\right)t \qquad 0 < t < d_1 T_s$$

$$i_{L3} = I_{i,W} + \frac{V_W}{L_3}t \qquad 0 < t < d_1 T_s$$

State III (M_1 off, M_2 on):

$$i_{L1} = I_{i,PV} + \left(\frac{V_{PV} - v_{c1}}{L_1}\right)t \qquad d_1 T_s < t < d_2 T_s$$

$$i_{L2} = I_{dc} + \frac{v_{c2}}{L_2}t \qquad d_1 T_s < t < d_2 T_s$$

$$i_{L3} = I_{i,W} + \frac{V_W}{L_3}t \qquad d_1 T_s < t < d_2 T_s$$

State IV (M_1 off, M_2 off):

$$i_{L1} = I_{i,PV} + \left(\frac{V_{PV} - v_{c1}}{L_1}\right)t \qquad d_2 T_s < t < T_s$$

$$i_{L2} = I_{dc} - \frac{V_{dc}}{L_2}t \qquad d_2 T_s < t < T_s$$

$$i_{L3} = I_{i,W} + \left(\frac{V_W - v_{c2} - V_{dc}}{L_3}\right)t \qquad d_2 T_s < t < T_s$$
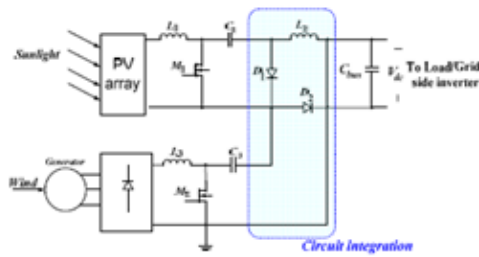
.

Fig 2: Proposed rectifier stage for a Hybrid wind/pv system
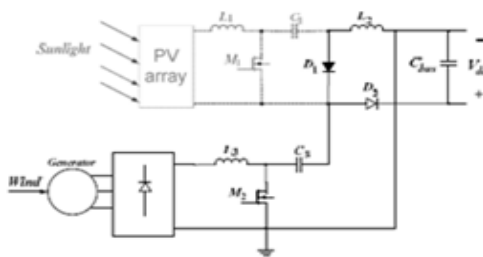
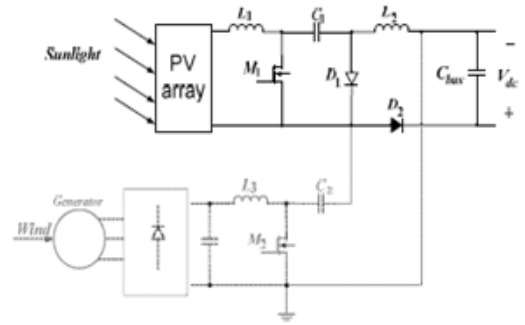

Fig 3: Only wind source is operational (SEPIC)

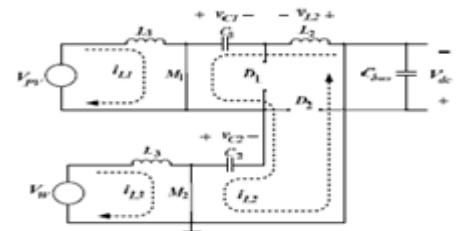Fig 4: Only PV source is operation (Cuk)
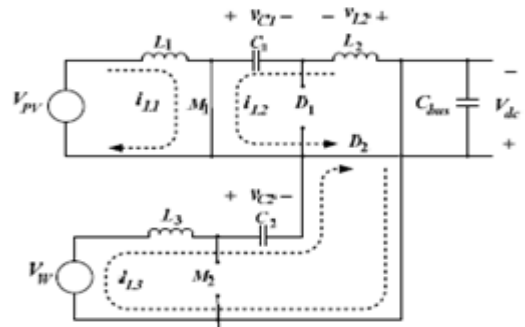

Fig 5 (I): M1 on, M2 on
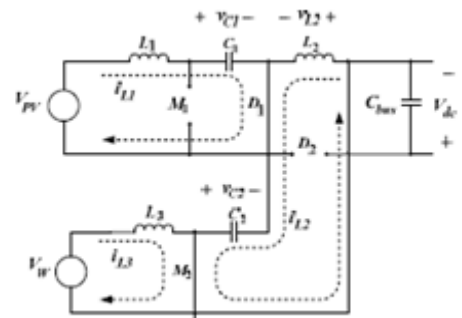

Fig 5 (II): M1 on, M2 off
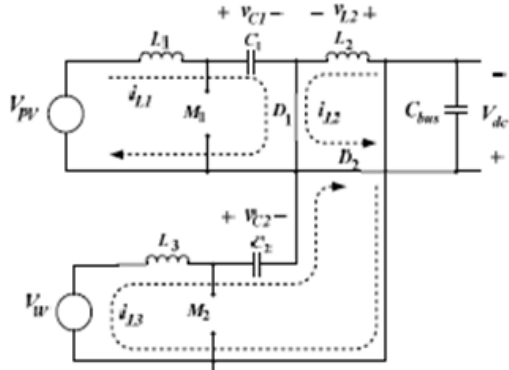

Fig 5 (III): M1 off, M2 on
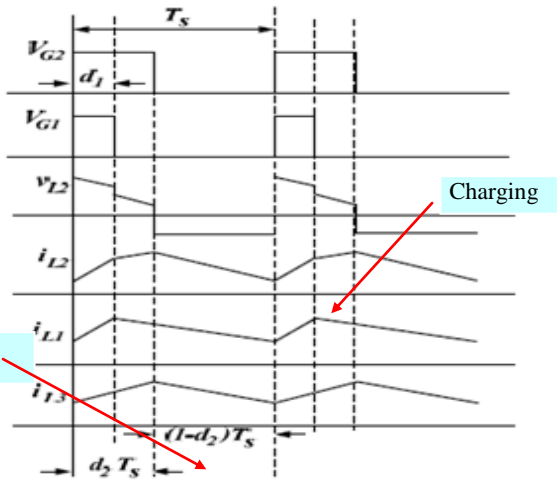
Fig 5 (IV): M1 off, M2 off

Fig 6: Proposed circuit inductor waveforms

III. ANALYSIS OF PROPOSED SYSTEM

To find an expression for the output DC bus voltage, Vdc, the volt-balance of the output inductor, L2, is examined according to Figure 6 with d2 > d1. Since the net change in the voltage of L2 is zero, applying volt-balance to L2 results in (3). The expression that relates the average output DC voltage (Vdc) to the capacitor voltages (vc1 and vc2) is then obtained as shown in (4), where vc1 and vc2 can then be obtained by applying volt-balance to L1 and L3. The final expression that relates the average output voltage and the two input sources (VW and VPV) is then given by (5). It is observed that Vdc is simply the sum of the two output voltages of the Cuk and SEPIC converter. This further implies that Vdc can be controlled by d1 and d2 individually or simultaneously.

$$(v_{c1} + v_{c2})d_1 T_s + (v_{c2})(d_2 - d_1)T_s + (1 - d_2)(-V_{dc})T_s = 0 \quad (3)$$

$$V_{dc} = \left(\frac{d_1}{1 - d_2}\right)v_{c1} + \left(\frac{d_2}{1 - d_2}\right)v_{c2} \quad (4)$$

$$V_{dc} = \left(\frac{d_1}{1 - d_1}\right)V_{PV} + \left(\frac{d_2}{1 - d_2}\right)V_w \quad (5)$$

The switches voltage and current characteristics are also provided in this section. The voltage stress is given by (6) and (7) respectively. As for the current stress, it is observed from Figure 6 that the peak current always occurs at the end of the on-time of the MOSFET. Both the Cuk and SEPIC MOSFET current consists of both the input current and the capacitors (C1 or C2) current. The peak current stress of M1 and M2 are given by (8) and (10) respectively. Leq1 and Leq2, given by (9) and (11), represent the equivalent inductance of Cuk and SEPIC converter respectively. The PV output current, which is also equal to the average input current of the Cuk converter, is given in (12). It can be observed that the average inductor current is a function of its respective duty cycle (d1). Therefore by adjusting the respective duty cycles for each energy source, maximum power point tracking can be achieved.

$$v_{ds1} = V_{pv}\left(1 + \frac{d_1}{1 - d_1}\right) \quad (6)$$

$$v_{ds2} = V_{W}\left(1 + \frac{d_2}{1 - d_2}\right) \quad (7)$$

$$i_{ds1,pk} = I_{i,PV} + I_{dc,avg} + \frac{V_{PV}d_1 T_s}{2L_{eq1}} \quad (8)$$

$$L_{eq1} = \frac{L_1 L_2}{L_1 + L_2} \quad (9)$$

$$i_{ds2,pk} = I_{i,W} + I_{dc,avg} + \frac{V_{W}d_2 T_s}{2L_{eq2}} \quad (10)$$

$$L_{eq2} = \frac{L_3 L_2}{L_3 + L_2} \quad (11)$$

$$I_{i,PV} = \frac{P_o}{V_{dc}}\frac{d_1}{1 - d_1} \quad (12)$$

IV. MPPT CONTROL OF PROPOSED CIRCUIT

A common inherent drawback of wind and PV systems is the intermittent nature of their energy sources. Wind energy is capable of supplying large amounts of power but its presence is highly unpredictable as it can be here one moment and gone in another. Solar energy is present throughout the day, but the solar

irradiation levels vary due to sun intensity and unpredictable shadows cast by clouds, birds, trees, etc. These drawbacks tend to make these renewable systems inefficient. However, by incorporating maximum power point tracking (MPPT) algorithms, the systems' power transfer efficiency can be improved significantly.

To describe a wind turbines power characteristic, equation (13) describes the mechanical power that is generated by the wind.

$$p_m = 0.5\rho A C_p(\lambda, \beta) v_w^3 \qquad (13)$$

Where
$\rho = air\ density,$
$A = rotor\ swept\ area,$
$C_p(\lambda, \beta) = power\ coefficient$
$\lambda = tip\ speed\ ratio,$
$\beta = pitch\ angle,$
$v_w = wind\ speed$

The power coefficient (Cp) is a nonlinear function that represents the efficiency of the wind turbine to convert wind energy into mechanical energy. It is dependent on two variables, the tip speed ratio (TSR) and the pitch angle. The TSR, λ, refers to a ratio of the turbine angular speed over the wind speed. The mathematical representation of the TSR is given by (14) [10]. The pitch angle, β, refers to the angle in which the turbine blades are aligned with respect to its longitudinal axis.

$$\lambda = \frac{R\ \omega_b}{v_w} \qquad (14)$$

Where
$R = turbine\ radius,$
$\omega b = angular\ rotational\ speed$

Figure 7 and 8 are illustrations of a power coefficient curve and power curve for a typical fixed pitch ($\beta =0$) horizontal axis wind turbine. It can be seen from figure 7 and 8 that the power curves for each wind speed has a shape similar to that of the power coefficient curve. Because the TSR is a ratio between the turbine rotational speed and the wind speed, it follows that each wind speed would have a different corresponding optimal rotational speed that gives the optimal TSR. For each turbine there is an optimal TSR value that corresponds to a maximum value of the power coefficient (Cp,max) and therefore the maximum power. Therefore by controlling rotational speed, (by means of adjusting the electrical loading of the turbine generator) maximum power can be obtained for different wind speeds.
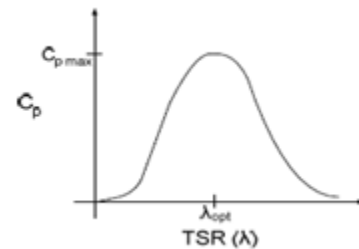

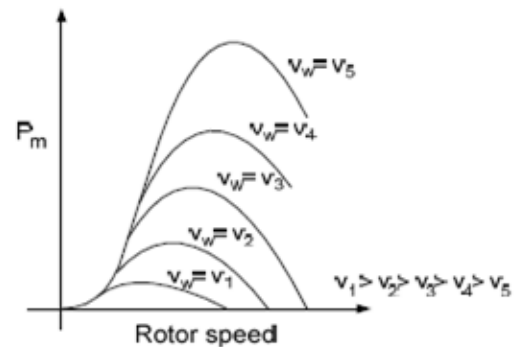Fig 7: Power Coefficient curve for a wind turbine

Fig 8: Power Curves for a typical wind turbine

A solar cell is comprised of a P-N junction semiconductor that produces currents via the photovoltaic effect. PV arrays are constructed by placing numerous solar cells connected in series and in parallel. A PV cell is a diode of a large-area forward bias with a photo voltage and the equivalent circuit is shown by Figure 9. The current-voltage characteristic of a solar cell is derived as follows:

$$I = I_{ph} - I_D \qquad (15)$$

$$I = I_{ph} - I_0 \left[\exp\left(\frac{q(V + R_s I)}{A k_B T} \right) - 1 \right] - \frac{V + R_s I}{R_{sh}} \qquad (16)$$

Where
$I_{ph} = photocurrent,$
$I_D = diode\ current,$
$I_0 = saturation\ current,$
$A = ideality\ factor,$
$q = electronic\ charge\ 1.6 \times 10\text{-}9,$
$k_B = Boltzmann's\ gas\ constant\ (1.38 \times 10^{-23}),$
$T = cell\ temperature,$
$R_s = series\ resistance,$
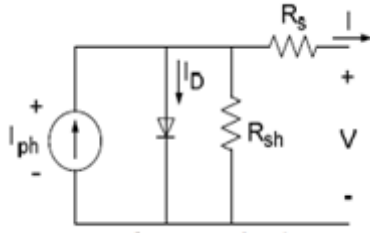$R_{sh} = shunt\ resistance,$
$I = cell\ current,$

Fig 9: PV cell equivalent characteristic

Typically, the shunt resistance (Rsh) is very large and the series resistance (Rs) is very small. Therefore, it is common to neglect these resistances in order to simplify the solar cell model. The resultant ideal voltage-current characteristic of a photovoltaic cell is given by (17) and illustrated by Figure 10.

$$I = I_{ph} - I_0 \left(\exp\left(\frac{qV}{kT}\right) - 1 \right) \qquad (17)$$
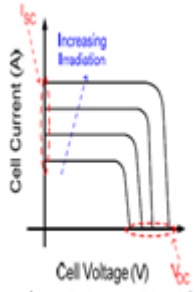

Fig 10: PV cell voltage-current characteristic

The typical output power characteristics of a PV array under various degrees of irradiation is illustrated by Figure 11. It can be observed in Figure 11 that there is a particular optimal voltage for each irradiation level that corresponds to maximum output power. Therefore by adjusting the output current (or voltage) of the PV array, maximum power from the array can be drawn.
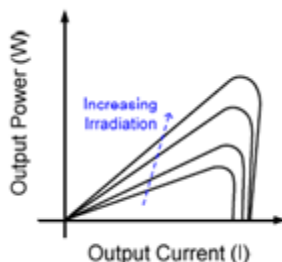

Fig 11: PV cell power characteristics

Due to the similarities of the shape of the wind and PV array power curves, a similar maximum power point tracking scheme known as the hill climb search (HCS) strategy is often applied to

these energy sources to extract maximum power. The HCS strategy perturbs the operating point of the system and observes the output. If the direction of the perturbation (e.g. an increase or decrease in the output voltage of a PV array) results in a positive change in the output power, then the control algorithm will continue in the direction of the previous perturbation. Conversely, if a negative change in the output power is observed, then the control algorithm will reverse the direction of the pervious perturbation step. In the case that the change in power is close to zero (within a specified range) then the algorithm will invoke no changes to the system operating point since it corresponds to the maximum power point (the peak of the power curves).

V. SINUSOIDAL PULSE WIDTH MODULATION

In the most straight forward implementation, generation of the desired output voltage is achieved by comparing the desired reference waveform (modulating signal) with a high frequency triangular 'carrier' wave as depicted schematically in Fig. 12. Depending on whether the signal voltage is larger or smaller than the carrier waveform, either the positive or negative dc bus voltage is applied at the output. Note that over the period of one triangle wave, the average voltage applied to the load is proportional to the amplitude of the signal (assumed constant) during this period. The resulting chopped square waveform contains a replica of the desired waveform in its low frequency components, with the higher frequency components being at frequencies of a close to the carrier frequency. Notice that the root mean square value of the ac voltage waveform is still equal to the dc bus voltage, and hence the total harmonic distortion is not affected by the PWM process. The harmonic components are merely shifted into the higher frequency range and are automatically filtered due to inductances in the ac system.

When the modulating signal is a sinusoid of amplitude Am, and the amplitude of the triangular carrier is Ac, the ratio m=Am/Ac is known as the modulation index. Note that controlling the modulation index therefor controls the amplitude of the applied output voltage. With a sufficiently high carrier frequency fc/fm = 21 and t = L/R = T/3; T = period of fundamental, the high frequency components do not propagate significantly in the ac network (or load) due the presence of the inductive elements. However, a higher carrier frequency does result in a larger number of switching's per cycle and hence in an increased power loss. Typically switching frequencies in the 2-15 kHz range are considered adequate for power systems applications. Also in three-phase systems it is advisable to use fc/fm=3k, (k∈N) so that all three waveforms are symmetric.
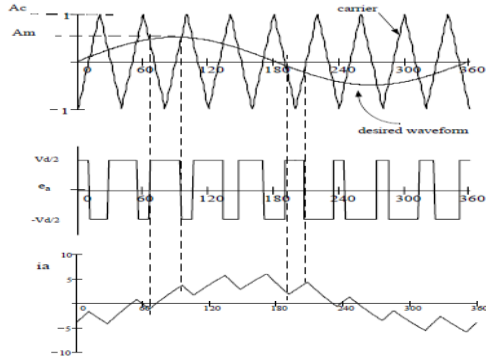
Fig 12: Principal of Pulse Width Modulation

Note that the process works well for. For, there are periods of the triangle wave in which there is no intersection of the carrier and the signal. However, a certain amount of this "over modulation" is often allowed in the interest of obtaining a larger ac voltage magnitude even though the spectral content of the voltage is rendered somewhat poorer. Note that with an odd ratio for fc/fm, the waveform is anti-symmetric over a 360 degree cycle. With an even number, there are harmonics of even order, but in particular also a small dc component. Hence an even number is not recommended for single phase inverters, particularly for small ratios of fc/fm.

VI. SIMULATION RESULTS

In this section, simulation results from MATLAB are given to verify that the proposed multi-input rectifier stage can support individual as well as simultaneous operation. The specifications for the design example are given in TABLE I. Figure 13 illustrates the hybrid wind solar simulation model. From figure 14 to figure 17 illustrates the outputs voltage of simultaneous and individual modes operation. Finally, Figure 18 illustrates the mppt operation with Cuk-SEPIC fusion mode of the two sources.

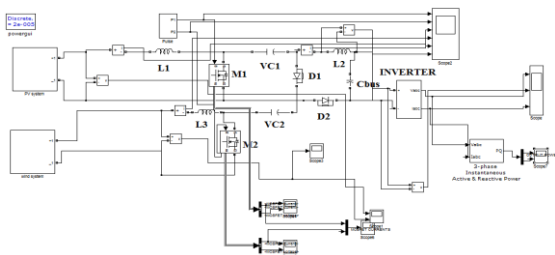| Output power (W)	3kW
Output voltage	500V
Switching frequency	20kHz

Table I: Design specifications

Fig.13 Hybrid wind solar model with cuk sepic converter

When the SEPIC operation is performed wind source is going to off and the solar source is talking place and producing supply to the load at the output of a inverter is placed in the circuit .the output of the inverter is shown in the fig .15 ,and the output of the wind and solar is shown in fig 12,14.here the wind output is AC and solar output is DC.As well as CUK operation also performed which shown in 17.In fig 13 and 16 the inductors L1 and L2 waveforms are shown for SEPIC and CUK operations.
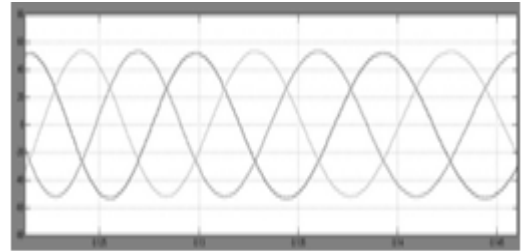

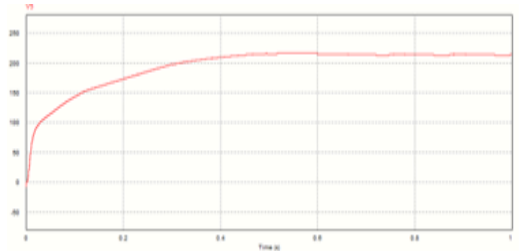Fig.14 Output voltage of hybrid Wind Solar with inverter

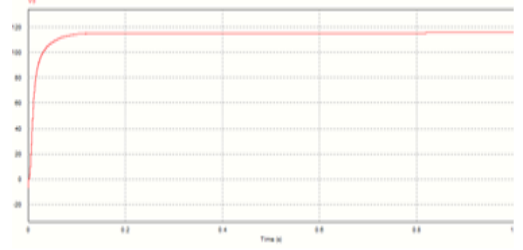Fig.15 Output voltage of both cuk sepic fusion converters

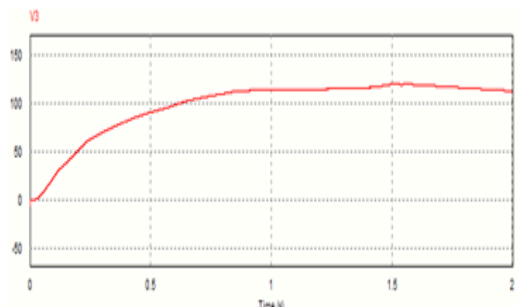Fig.16 Output voltage of solar alone (cuk mode)

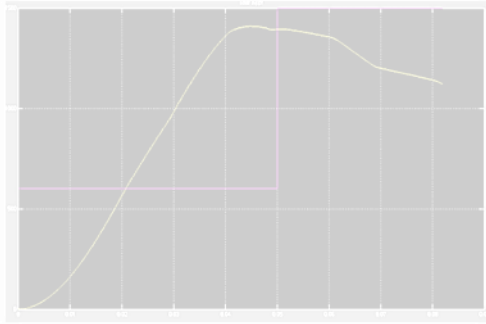Fig.17 Output voltage of wind alone (sepic mode)

Fig.18 MPPT controller of pv and wind sources

VII. CONCLUSION

In this paper a new multi-input Cuk-SEPIC rectifier stage for hybrid wind/solar energy systems has been presented. The features of this circuit are: 1) additional input filters are not necessary to filter out high frequency harmonics; 2) both renewable sources can be stepped up/down (supports wide ranges of PV and wind input); 3) MPPT can be realized for each source; 4) individual and simultaneous operation is supported. Simulation results have been presented to verify. Here he represented a sinusoidal pulse width modulation for the inverter .It will provide a better output results for the load.

REFERENCES

[1] S.K. Kim, J.H Jeon, C.H. Cho, J.B. Ahn, and S.H. Kwon, "DynamicModeling and Control of a Grid-Connected Hybrid Generation System with Versatile Power Transfer," IEEE Transactions on Industrial Electronics, vol. 55, pp. 1677-1688, April 2008.

[2] D. Das, R. Esmaili, L. Xu, D. Nichols, "An Optimal Design of a Grid Connected Hybrid Wind/Photovoltaic/Fuel Cell System for Distributed Energy Production," in Proc. IEEE Industrial Electronics Conference, pp. 2499-2504, Nov. 2005.

[3] N. A. Ahmed, M. Miyatake, and A. K. Al-Othman, "Power fluctuations suppression of stand-alone hybrid generation combining solar photovoltaic/wind turbine and fuel cell systems," in Proc. Of Energy Conversion and Management, Vol. 49, pp. 2711-2719, October 2008.

[4] S. Jain, and V. Agarwal, "An Integrated Hybrid Power Supply for Distributed Generation Applications Fed by Nonconventional Energy Sources," IEEE Transactions on Energy Conversion, vol. 23, June 2008.

[5] Y.M. Chen, Y.C. Liu, S.C. Hung, and C.S. Cheng, "Multi-Input Inverter for Grid-Connected Hybrid PV/Wind Power System," IEEE Transactions on Power Electronics, vol. 22, May 2007.

[6] dos Reis, F.S., Tan, K. and Islam, S., "Using PFC for harmonic mitigation in wind turbine energy conversion systems" in Proc. of the IECON 2004 Conference, pp. 3100- 3105, Nov. 2004

[7] R. W. Erickson, "Some Topologies of High Quality Rectifiers" in the Proc. of the First International Conference on Energy, Power, and Motion Control, May 1997.

Authors

N.V.S Rakesh Kumar was born in Hyderabad, India, in 1989. He received the B.TECH in GLOBAL COLLEGE OF ENG. & TECH. from the UNIVERSITY OF JNTU, Hyderabad, in 2010 and the M.TECH in CMR COLLEGE OF ENG. & TECH from the UNIVERSITY OF JNTU, Hyderabad, in 2012. His research interests include power electronics, environmental studies, and power quality

Mr. G.Devadas is currently working as Professor, Electrical & Electronics Engineering in the Department of EEE, CMR College of Engineering & Technology, Kandlakoya, and Hyderabad. He obtained his B.Tech degree in 1997 from NAGARJUNA UNIVERSITY and M.Tech degree in 2002 with a specialization in Power Systems and Automation from ANDHRA UNIVERSITY, VISAKHAPATNAM, INDIA. He had 13 years of teaching experience. During his teaching career he taught various subjects like Electrical Machines, Power Systems and Control Systems, etc. His research interests include Power Quality, Wavelet Transforms, and Neural & Fuzzy expert Systems.

Mr. K.Chandrashekar Reddy is currently working as Assistant Professor, Electrical & Electronics Engineering in the Department of EEE, and CMR College of Engineering & Technology, Kandlakoya, and Hyderabad. He obtained his B.Tech degree in 2007 from BANDARI SRINIVAS INSTITUTE OF ENG. & TECH. and M.Tech degree in 2009 with a specialization In Embedded Systems. He had 3 years of teaching experience. During his teaching career he taught various subjects like Power Electronics, Uee, Mpmc, and Embedded Systems. His research interests include power electronics and embedded systems.